Three/Four-leg Inverter Current Control Based on Generalized Symmetrical Components

E. V. Liberado
Group of Automation and Integrated Systems
São Paulo State University
Sorocaba, Brazil
evldoc@dsce.fee.unicamp.br

A. M. S. Alonso
Group of Automation and Integrated Systems
São Paulo State University
Sorocaba, Brazil
augusto.alonso@unesp.br

F. P. Marafão
Group of Automation and Integrated Systems
São Paulo State University
Sorocaba, Brazil
fernando.marafao@unesp.br

J. A. Pomilio
Dept. of Systems and Energy
University of Campinas
Campinas, Brazil
antenor@dsce.fee.unicamp.br

E. Tedeschi
Dept. of Electric Power Engineering
Norwegian Univ. of Science and Technology
Trondheim, Norway
elisabetta.tedeschi@ntnu.no

J. F. Guerreiro
Dept. of Systems and Energy
University of Campinas
Campinas, Brazil
joel.engeletrica@gmail.com

***Abstract*—Considering a scenario of high penetration of voltage source inverters in distribution grids, on which the number of conductors is variable, this paper proposes a current control approach for three- or four-leg inverters based on the generalized symmetrical components decomposition of non-sinusoidal signals. The approach is an alternative to $d-q$ and $\alpha-\beta$ transformation-based approaches and allows to model and design the control system directly in the abc frame. Simulation results of three- and four-leg inverters operating as multifunctional interfaces of distributed energy resources are presented, as well as comparative results of the proposed approach and other abc frame-based approaches to control four-leg inverters.**

***Index Terms*—control of power converters, switching power interface, distributed energy resources, multifunctional power converter, generalized symmetrical components**

I. Introduction

High penetration of voltage source inverters (VSIs) in distribution systems is a trending topic in the grid modernization [1], [2], since they act as Switching Power Interfaces (SPIs) [3] for Distributed Energy Resources (DERs) such as the photovoltaic (PV) and wind plants [4]. Due to its capacity to synthesize any controlled voltage or current waveform, the SPI allows the multifunctional operation of DERs, which can therefore perform a variety of ancillary services apart from active power generation, like reactive power control, voltage regulation and power quality improvement [5]–[8].

At low voltage distribution systems, the number of conductors at the DER point of connection with the grid may vary as there are four, three or two-wire systems, thus the number of legs in the SPI may vary as well.

This work was supported by the São Paulo Research Foundation (FAPESP) under grants 2016/08645-9 and 2017/24652-8; by the National Council for Scientific and Technological Development (CNPq) under grant 302257/2015-2 and by the Research Council of Norway under grant f261735/H30.

Regarding the three- or four-leg VSIs, their control variables (voltages or currents) are cross-coupled in the abc frame, as verified in [9]. Hence, a VSI with N legs cannot impose N independent currents (or voltages).

Even in the three-phase three-wire case with absence of zero-sequence component, when attempting to control three currents or voltages, the sensors and signal conditioning boards may introduce zero-sequence or offset in the measured signals. These disturbances may lead the inverter control to unstable conditions. Instead, in the four-wire case, a three-leg VSI with neutral point clamped [10] can operate as three single-phase inverters and then control three independent variables [11].

On the other hand, a general approach for a N-leg VSI ($N = 2,\ 3,\ 4$) consists in controlling only $N-1$ variables. For $N = 3,\ 4$, this can be achieved by applying coordinate transformations (e.g., $\alpha-\beta$ [12] and/or $d-q$ [9]) to the control variables in the abc frame and designing the controllers considering the control variables of the alternative frame. In fact, the coordinate transformation to the $\alpha-\beta$ frame results in a system with orthogonal components and the voltages and currents are decoupled [12]. On $d-q$ frame the voltage components are coupled to the corresponding currents, but a decoupling method is available [9].

Alternatively, for $N = 3,\ 4$, schemes to model $N-1$ controllers directly in the abc frame have been also presented. Holmes *et al.* [13] propose a zero-sequence-like signal to be summed to the Pulse-Width-Modulation (PWM) input signals of the N inverter legs, which results in the sum of the N inverter output signals being instantaneously zero. Moreover, Matakas *et al.* [11], [14] propose an optimum zero-sequence signal, on which the phase-connected inverter legs would have balanced output signals.

Therefore, this paper presents a new approach for three-

and four-leg VSI current control based on the generalized symmetrical components (GSC) decomposition [15], which is re-issued in section II. The main difference of the proposed approach in relation to the abc frame-based ones mentioned previously [13], [14] is that the abc frame variables are decoupled during the current reference signal generation by decomposing it in homopolar and heteropolar components. Also, it is proposed that the VSI non-controlled leg is a phase-connected one, instead of not controlling the neutral-connected in the four-leg VSI [13], [14].

Moreover, some advantages of the GSC decomposition in relation to the coordinate transformations are: 1) it does not change the harmonic orders present in the abc frame signals, hence the current controllers (which in this paper are proportional-resonant ones) for the VSI controlled legs are designed considering the harmonic orders in the abc frame; 2) it does not require the application of synchronization algorithms (e.g., the phase-locked loop) as needed in the $d-q$ frame-based approaches [16], which reduces the implementation complexity.

Thus, section III presents a GSC decomposition-based control strategy that allows active power injection and power quality improvement functions for N-leg VSIs ($N = 3,\ 4$). Simulation results are presented in section V and include comparisons between the proposed approach and the conventional abc frame ones [13], [14], which are briefly described in section IV.

II. Signal decomposition in homopolar and heteropolar components

The generalized symmetrical components (GSC) were defined in [15]. They consist in a time domain approach to decompose periodic non-sinusoidal three-phase signals into positive-sequence, negative-sequence, zero-sequence and residual components. Their relationship with the Fortescue's symmetrical components were analyzed in [17].

For the following definitions, consider a three-phase four-wire system on which $u_1,\ u_2,\ u_3$ are the phase-neutral voltages, $i_1,\ i_2,\ i_3$ are the phase currents and i_4 the current in the neutral conductor (all instantaneous quantities).

Thus, the zero-sequence component (also called homopolar component, denoted by ^{ho}) defined in [15] is calculated for the non-sinusoidal signals in a similar way as the Forstescue's zero-sequence calculated for each frequency:

$$u^{ho} = \frac{1}{3}\cdot\sum_{n=1}^{3} u_n, \quad i^{ho} = \frac{1}{3}\cdot\sum_{n=1}^{3} i_n = -\frac{i_4}{3},\ n = 1,2,3. \quad (1)$$

The heteropolar components (denoted by ^{he}) are calculated by subtracting the homopolar component from the original signals, as shown in 2. They are composed by positive-sequence, negative-sequence and residual components.

$$u_n^{he} = u_n - u^{ho}, \quad i_n^{he} = i_n - i^{ho},\ n = 1,2,3. \quad (2)$$

Regarding the residual components, they are composed by harmonic orders that are multiple of 3 and unbalanced. Also, they are typically observed in three-phase three-wire systems.

An interesting characteristic of the three-phase heteropolar components is that their instantaneous sum results zero, i.e.,

$$\sum_{n=1}^{3} i_n^{he} = 0. \quad (3)$$

Therefore, from a set of three control variables composed by heteropolar components, just two variables are controlled since the third one is linearly-dependent on the others.

Moreover, the quantities of a three-phase three-wire system (phase-to-phase voltages and phase currents) are composed only by heteropolar components.

III. Control strategy based on homopolar and heteropolar components

Fig. 1 presents a 20 kVA four-leg inverter operating as a SPI of a generic DER represented by a dc current source. The dc current is a function of the active power to be generated (P_{ER}) and the dc-link voltage (U_{DC}). A LCL filter designed as proposed in [18] connects the DER to the point of common coupling (PCC) between a consumer and the grid.

For the four-leg inverter, the proposed control strategy consists in controlling the currents of two phase-connected legs and also the current of the neutral-connected leg. Also, only the currents injected by the phase-connected legs are measured (the fourth leg current can be obtained from them) and their heteropolar components feedback the current references of the two phase-connected controlled legs. The proportional-resonant controller (G_{PR}) is adopted in order to obtain zero steady state error in selected harmonic frequencies.

Since the instantaneous sum of the heteropolar components is zero, the PWM input signal of the third leg is obtained from the two phase-connected controlled legs, thus

$$u_{C,3}^{ref} = -\left(u_{C,1}^{ref} + u_{C,2}^{ref}\right), \quad (4)$$

as shows Fig. 1.

Fig. 2 presents a simple approach to generate the reference signals ($i_{SPI,1}^{ref}, i_{SPI,2}^{ref}, i_{SPI,4}^{ref}$) for the controlled legs of the SPI. This approach is just intended for evaluating the control strategy proposed (Fig. 1). A more complex reference signal generation approach that considers selective disturbance compensation and/or DER ancillary services can be defined in future works.

The dc link voltage U_{DC} is regulated by a proportional-integral controller (G_{PI}). The output of G_{PI} gives the conductance that is proportional to the active power to be generated and it prevents the SPI from consuming active power from the grid when operating as active filter. Moreover, the use of heteropolar voltages assures the active power injection only through the phase-connected legs.

The active filtering function aims at improving the power quality at the DER point of connection with the grid by compensating all the non-active components of the load currents and thus maximizing the power factor at the PCC [5]. This is made by removing the current component that corresponds to active power consumption from $i_{cons,1},\ i_{cons,2},\ i_{cons,3}$. That

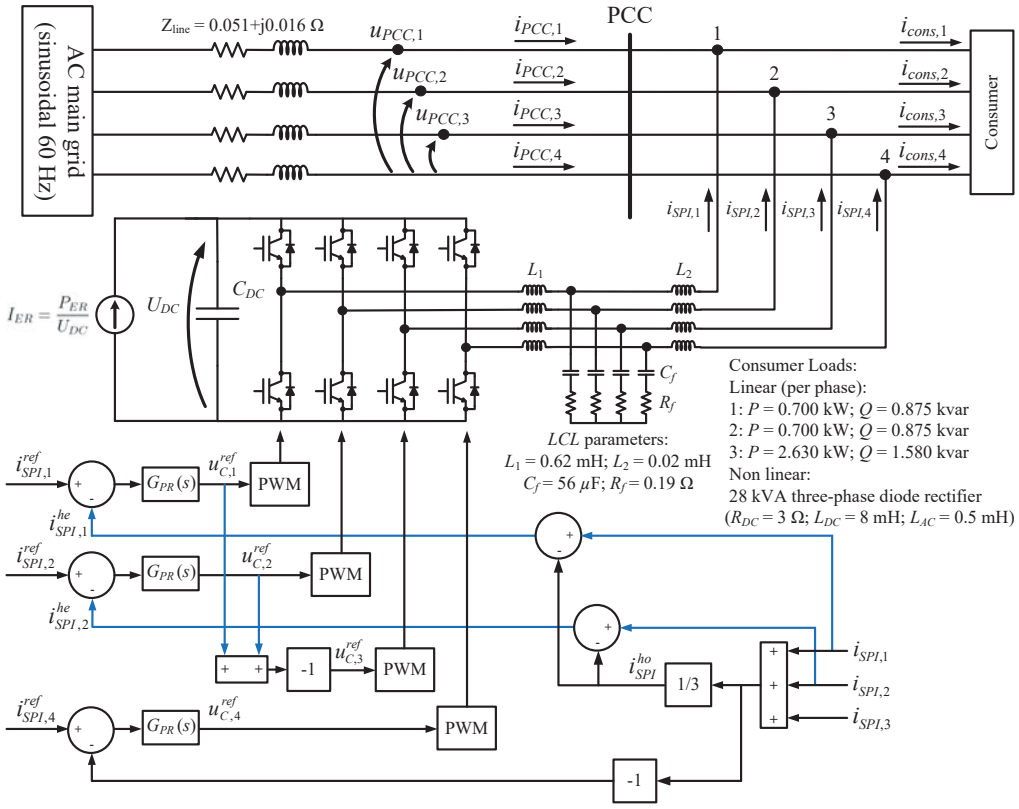

Fig. 1. Four-leg inverter connected to a low voltage distribution grid and its current control loop.

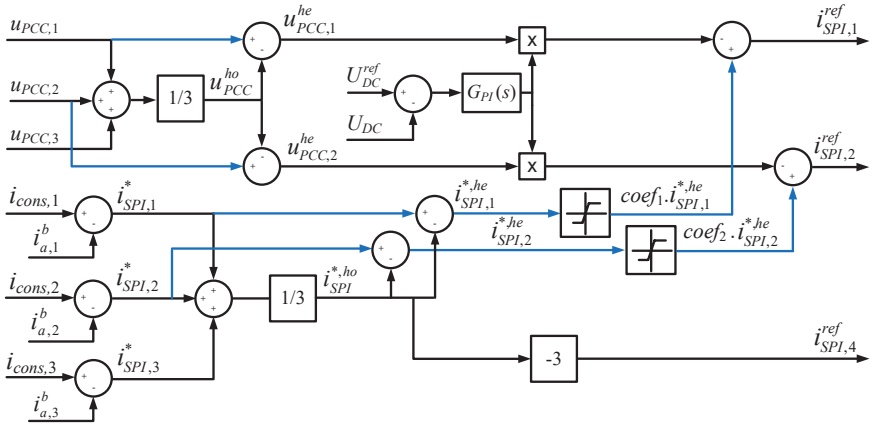

Fig. 2. Reference signal generation for active power injection and power quality improvement.

current component is called balanced active current [19] and is calculated for three-phase systems as:

$$i^{b}_{a,n} = \frac{P_{cons}}{U^2_{PCC,1} + U^2_{PCC,2} + U^2_{PCC,3}} \cdot u_{PCC,n}, \qquad (5)$$

on which P_{cons} is the three-phase active power consumed by the load, $U_{PCC,1}$, $U_{PCC,2}$ $U_{PCC,3}$ are the rms values of the PCC line-neutral voltages and $n = 1,\ 2,\ 3$.

The resulting signals $\left(i^{*}_{SPI,1},\ i^{*}_{SPI,2},\ i^{*}_{SPI,3}\right)$ are decomposed in homopolar and heteropolar components, which are addressed to compose the reference signals of the neutral-connected leg and the controlled phase-connected legs, respectively.

Assuming that the active power injection has the highest priority in relation to the active filtering function, a saturation strategy should be defined. Since no active power is injected through the fourth leg, its operation could be limited just by the nominal current injection capacity of the inverter. Also, by limiting the active power injected to the inverter power capacity (in this case, 20 kVA), the following saturation algo-

rithm can be applied for the two phase-connected controlled legs:

$A^{*,he}_{SPI,n} = U^{he}_{PCC,n} \cdot I^{*,he}_{SPI,n}$

$A^{av}_{SPI,n} = \sqrt{(20\text{ k}/3.0)^2 - (P^b_n)^2}$

if $A^{*,he}_{SPI,n} > A^{av}_{SPI,n}$ **then**

$coef_n \leftarrow \frac{A^{av}_{SPI,n}}{A^{*,he}_{SPI,n}}$

else

$coef_n \leftarrow 1.0$

end if

In this algorithm, $n = 1,\ 2$; $A^{*,he}_{SPI,n}$ is the power that corresponds to the non-active heteropolar current that should be compensated by the leg n; $A^{av}_{SPI,n}$ is the available power for compensation in the leg n, calculated considering the inverter nominal power and the active power to be injected by each phase-connected leg $\left(P^b_n\right)$, which is calculated as:

$$P^b_n = \frac{P_{ER}}{U^2_{PCC,1} + U^2_{PCC,2} + U^2_{PCC,3}} \cdot U^2_{PCC,n},\ n = 1, 2. \quad (6)$$

Thus, if $A^{*,he}_{SPI,n} \geq A^{av}_{SPI,n}$, the coefficient $coef_n$ is calculated in order to limit the corresponding current $i^{*,he}_{SPI,n}$, as shown in Fig. 2.

Finally, the control strategy and signal reference generation described in this section are also valid for the three-leg inverter connected to the three phases of a three or four-wire grid, as will be discussed in section V.

IV. Conventional schemes to use $N-1$ controllers in the abc frame

Fig. 3 presents the approaches proposed by Holmes *et al.* [13] and Matakas *et al.* [14] to use $N-1$ controllers designed directly in the abc frame to control the four-leg inverter depicted in Fig. 1.

In both schemes, the reference signal for the PWM of the fourth leg is function of the controlled legs, which are connected to the grid phases. Moreover, no GSC decomposition is used (note that the currents that feedback the controlled legs are the measured ones).

In the scheme of Fig. 3(a), the PWM input signal of the fourth-leg is calculated as

$$u^{ref}_{C,4} = -\frac{u^*_{C,1} + u^*_{C,2} + u^*_{C,3}}{3}, \quad (7)$$

which is indeed a homopolar signal that is summed to the PWM reference signals of the phase-connected legs. This operation results that the sum of PWM input signals of the four legs equals to zero.

In the scheme proposed in [14],

$$u^{ref}_{C,4} = u^*_{C,4} + u_{z-opt}, \quad (8)$$

on which $u^*_{C,4} = -\left(u^*_{C,1} + u^*_{C,2} + u^*_{C,3}\right)$ and u_{z-opt} is the optimum zero-sequence signal, defined as

$$u_{z-opt} = -\frac{\min\left(u^*_{C,m}\right) + \max\left(u^*_{C,m}\right)}{2}, \quad (9)$$

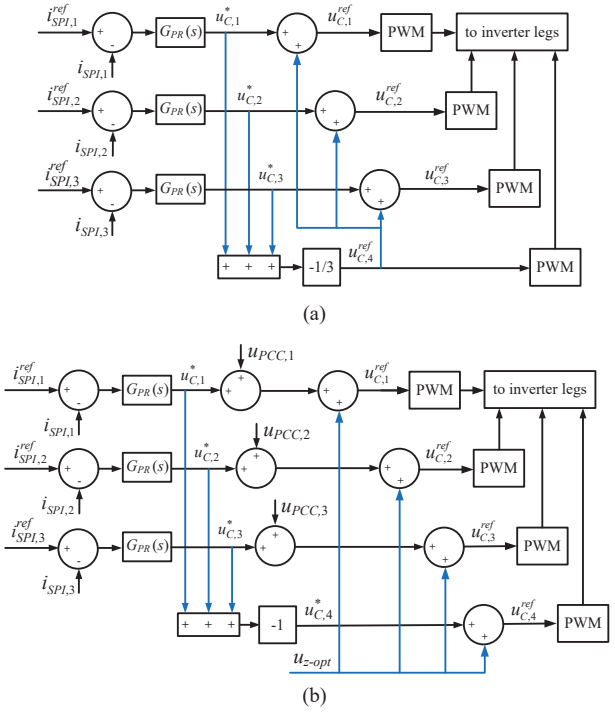

Fig. 3. Control strategies based on the schemes proposed by (a) [13] (b) [14].

for $m = 1,\ 2,\ 3,\ 4$. If $u^{ref}_{C,4} = u_{z-opt}$, instead of using (8), the term u_{z-opt} would reduce the amplitude of the PWM input signals of the phase-connected legs in comparison with the other approaches. However, by using (8) the PWM input signals of the controlled legs will be decoupled and the four-leg inverter will be equivalent to three single-phase two-leg inverters.

An additional feature of the control strategy based on [14] is that the grid voltages feedforward the corresponding controller outputs, which reduce the influence of disturbances present in the grid voltages on the inverter outputs.

V. Simulation results

In the following results, the grid presented in Fig. 1 is simulated using PSIM® with sinusoidal 60 Hz, positive-sequence, 220 V phase-to-phase supply voltages. Two inverter topologies are simulated: the four-leg inverter and the three-leg inverter connected to the three grid phases. The reference value for the dc link voltage control U^{ref}_{DC} is 600 V and G_{PI} is designed considering a natural frequency equal to 20 Hz and phase margin equal to 70°. The current controller G_{PR} is designed in such a way that the open-loop transfer function of the control system has unitary magnitude at the crossover frequency (1200 Hz). Also, the resonant gains are designed for the fundamental frequency plus the 5^{th} and 7^{th} harmonic orders. These gains are functions of G_{PR} proportional gain and the desired transient response time (1/60 s) [12]. Simulation total time 1 s and the sampling frequency is 12 kHz.

A. Case 1: Four-leg inverter

In this case, the DER is set to generate 15 kW, thus the four-leg SPI can also perform power quality improvement at PCC, since its nominal power is 20 kVA.

Fig. 4 presents the PCC phase-neutral voltages, load currents, currents at the PCC, currents injected by the inverter legs and their corresponding PWM input signals. The load currents have a quasi-square wave shape due to the three-phase diode rectifier with inductive dc load. Also, the neutral current is sinusoidal because the linear loads are unbalanced. However, due to the active filtering action of the SPI, the phase currents at PCC have a sinusoidal shape with high order harmonic components while the neutral current is compensated by the SPI. Regarding the PWM input signals, note that the ones of the phase-connected legs are balanced and composed by positive and negative-sequence signals. The neutral-connected leg signal is as low as the neutral current in relation to the phase currents.

Fig. 4 also shows the dc link voltage behavior in the beginning of the simulation. The dc voltage reference value is gradually increased until reach the 600 V, thus U_{DC} smoothly converges to the desired value due to the control action. After the dc voltage convergence ($t = 0.2$ s) the SPI starts to perform active power injection and active filtering functions.

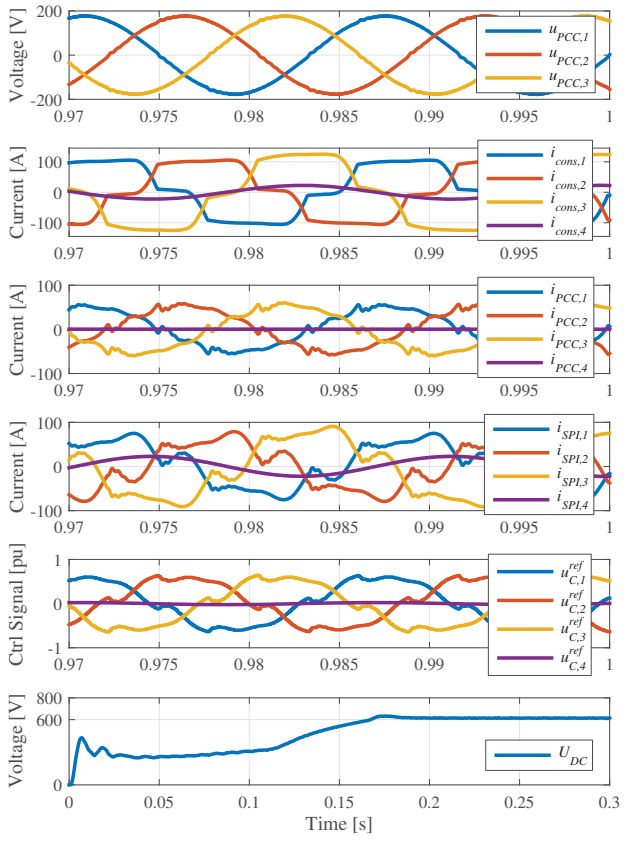

Fig. 4. Waveform results of simulation case 1.

The values of active power injected and the power quality indices of this case are presented in Table I and discussed together with the next case.

B. Case 2: Three-leg phase-connected inverter

For this case, the same four-wire grid of Fig. 1 is used. The three-leg inverter has the same control loops of the phase-connected legs of the four-leg inverter, and $u_{C,3}^{ref}$ is calculated using (4). The DER is also set to generate 15 kW.

Thus, Fig. 5 presents the waveform results of this simulation. The phase currents at PCC are very similar to the ones from the previous case, and the neutral current is not compensated because the current references $i_{SPI,1}^{ref}$, $i_{SPI,2}^{ref}$ (and consequently the PWM input signals) are composed only by heteropolar components.

Table I presents apparent and active power values at the PCC and injected by the SPI, as well as two power quality indices (power factor - PF - and the total harmonic distortion of phase currents - THD_i) at the PCC for simulations without the DER and the two cases previously described. In both cases with the DER the PCC power quantities are reduced and the power factor is close to unity, which indicates that the proposed active filtering function aims at maximizing the power factor at the PCC. Both SPIs injected the pre-defined active power value and their apparent power is slightly lower than the nominal one (20 kVA). Also, the saturation coefficients were unitary in both cases.

In addition, note that the sum of the active power at the PCC and the one generated by the DER is slightly higher than in the grid without DER, which indicates an increasing in the voltage magnitudes at the PCC due to the active power injected by the DER.

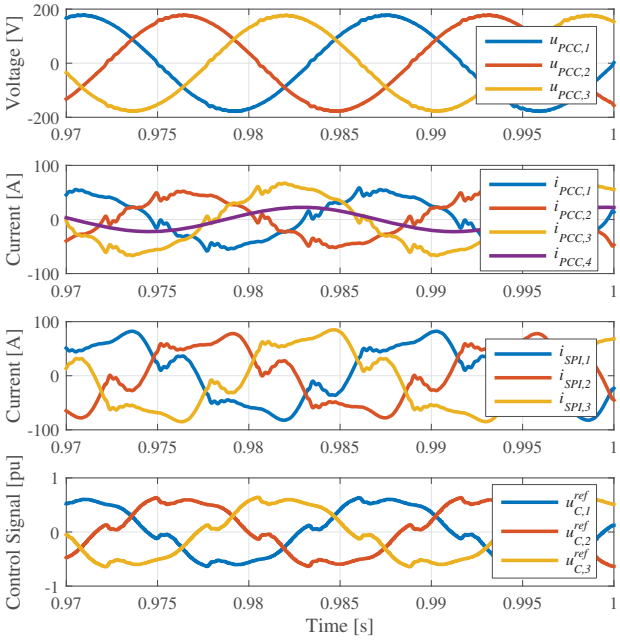

Fig. 5. Waveform results of simulation case 2.

TABLE I
PCC AND SPI POWER QUANTITIES AND POWER QUALITY INDICES IN THE GRID WITHOUT AND WITH DER.

	without DER	**DER with 4-leg SPI**	**DER with 3-leg SPI**
PCC power quantities and power quality indices			
A [kVA]	30.792	14.383	14.512
P [kW]	28.048	14.284	14.273
PF	0.910	0.993	0.983
$THD_{i,1}$ [%]	18.335	10.844	11.090
$THD_{i,2}$ [%]	18.335	10.371	11.565
$THD_{i,3}$ [%]	15.269	10.245	9.091
$THD_{i,4}$ [%]	0.445	0.000	0.117
SPI power quantities			
A [kVA]		19.607	19.509
P [kW]		15.016	15.019

C. Case 3: Comparison among control strategies for the four-leg inverter

The grid and DER of Fig. 1 is simulated with three different control strategies for the four-leg inverter: the control strategy based on the GSC decomposition (denoted as *a1*) and the ones based on the schemes proposed by Holmes *et al.* (denoted as *a2*) and Matakas *et al.* (denoted as *a3* in the following results).

In the three simulations, no active power is generated by the DER ($P_{ER} = 0$) and its SPI is just performing the active filtering function. Additionally, the same controllers are used and no GSC decomposition is applied in the current references generation in cases *a2* and *a3* (even in the dc link voltage control, on which the measured voltages are used instead).

Thus, Fig. 6 presents the voltages at the PCC and the resulting current at the PCC and injected by the four-leg inverter. The load currents are the same as presented in Fig. 4. Since the three simulations presented the same compensation results, the waveforms of the corresponding currents are superposed in Fig. 6. Moreover, the currents at PCC are less distorted than when the inverter was injecting active power, and the neutral current is completely compensated in the three cases.

Fig. 7 presents the PWM input signals from the three simulations. One can observe that approaches *a1* and *a2* have identical PWM input signals.

In fact, both approaches use sequence component-based decompositions and differ only by the way the signal that is decomposed: while in the approach *a2* the decomposition is applied to the PWM input signals, in approach *a1* the GSC decomposition is applied to the current reference signals.

Regarding approach *a3*, which resulted in four different PWM inputs in comparison with cases *a1* and *a2*, note that $u_{C,4}^{ref,a3}$ has the same envelope of $u_{C,4}^{ref,a1}$ and $u_{C,4}^{ref,a2}$ due to the first term of (8). In addition, term u_{z-opt} distributes the harmonic components in a different way than the other approaches, which explains the differences in the resulting waveforms for this approach.

Finally, Table II presents the power quantities and power

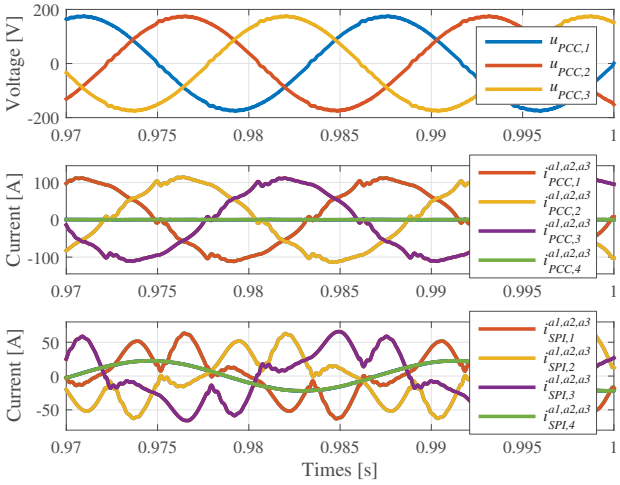

Fig. 6. Voltages and currents at the PCC and currents injected by the inverter from the simulations *a1*, *a2* and *a3*.

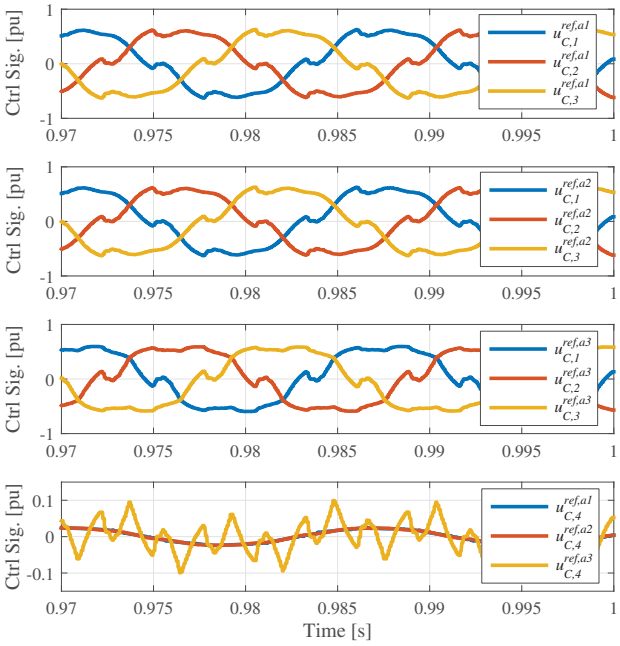

Fig. 7. PWM input signals of the simulations *a1*, *a2* and *a3*.

quality indices at the PCC and the apparent power injected by the inverter in the three simulations plus the case without the DER.

Similarly to the waveform results, the quantities presented in Table II show that the control strategies based on the three approaches compared in this paper have achieved identical results. The currents total harmonic distortion is lower than in the previous cases, since the inverter is not injecting active power and thus the active power flow at the PCC (and consequently the corresponding fundamental frequency current components) remains almost equal to the case without the DER. Additionally, the apparent power injected by the inverter operating as active filter corresponds to the non-active

TABLE II
PCC POWER QUANTITIES AND POWER QUALITY INDICES AND SPI APPARENT POWER IN THE GRID WITHOUT AND WITH DER.

	without DER	*a1*	*a2*	*a3*
PCC power quantities and power quality indices				
A [kVA]	30.792	28.433	28.432	28.435
P [kW]	28.048	28.393	28.329	28.393
PF	0.910	0.998	0.996	0.998
$THD_{i,1}$ [%]	18.335	5.001	4.994	5.154
$THD_{i,2}$ [%]	18.335	4.979	4.990	5.088
$THD_{i,3}$ [%]	15.269	4.957	4.954	5.088
$THD_{i,4}$ [%]	0.445	0.000	0.000	0.000
SPI power quantities				
A [kVA]		12.763	12.765	12.765

components of the load currents, from which the compensation has led the power factor to be almost unitary.

VI. CONCLUSION

This paper presented a new approach to control three and four-leg inverters using $N-1$ current controllers ($N = 3,\ 4$) designed directly in the abc frame. This approach applies the generalized symmetrical components (GSC) decomposition in the reference currents generation and addresses the heteropolar components of the currents to the phase-connected inverter legs and the homopolar components to the neutral-connected leg.

The proposed approach was tested in simulation of three and four-leg inverters operating as switching power interfaces of a DER, and the results shown effective injection of active power and active filtering functionality by the inverters. Comparative results of the proposed approach and two conventional abc frame-based approaches were also presented. Even though the reference currents and PWM input signals were different, the three approaches achieved identical results for the four-leg inverter operating as active filter.

However, an advantage of decomposing the control variables reference (in the presented cases, the currents) using the GSC instead of decoupling the PWM input signals only is that the GSC decomposition can be also used to define and model a variety of functionalities for the VSI inverter directly in the abc frame (e.g., voltage source operation that supplies positive-sequence voltages, series active filtering functions, load imbalance compensation etc.). These applications, as well as the application of the proposed approach in a three-leg two-phase+neutral-connected inverter [20], and additional discussion in relation to coordinate transformation-based approaches, can be presented in future works.

REFERENCES

[1] J. R. Aguero, E. Takayesu, D. Novosel, and R. Masiello, "Modernizing the grid: Challenges and opportunities for a sustainable future," *IEEE Power Energy Mag.*, vol. 15, no. 3, pp. 74–83, May 2017.

[2] F. Katiraei, C. Sun, and B. Enayati, "No inverter left behind: Protection, controls, and testing for high penetrations of pv inverters on distribution systems," *IEEE Power and Energy Magazine*, vol. 13, no. 2, pp. 43–49, March 2015.

[3] A. Costabeber, P. Tenti, T. Caldognetto, and E. V. Liberado, "Selective compensation of reactive, unbalance, and distortion power in smart grids by synergistic control of distributed switching power interfaces," in *Proc. of 15th European Conference on Power Electronics and Applications (EPE)*, Lille, France, Sep. 2013, pp. 1–9.

[4] F. Blaabjerg, Y. Yang, and K. Ma, "Power electronics - key technology for renewable energy systems - status and future," in *Proc. 3rd International Conference on Electric Power and Energy Conversion Systems EPECS*, Istanbul, Turkey, Oct. 2013, pp. 1–6.

[5] J. P. Bonaldo, H. K. M. Paredes, and J. A. Pomilio, "Control of single-phase power converters connected to low-voltage distorted power systems with variable compensation objectives," *IEEE Trans. Power Electron.*, vol. 31, no. 3, pp. 2039–2052, Mar. 2016.

[6] P. Tenti, T. Caldognetto, S. Buso, and A. Costabeber, "Control of utility interfaces in low voltage microgrids," in *Proc. of IEEE 5th International Symposium on Power Electronics for Distributed Generation Systems (PEDG)*, Jun. 2014, pp. 1–8.

[7] X. Wang, F. Blaabjerg, and Z. Chen, "Synthesis of variable harmonic impedance in inverter-interfaced distributed generation unit for harmonic damping throughout a distribution network," *IEEE Trans. Ind. Appl.*, vol. 48, no. 4, pp. 1407–1417, Jul./Aug. 2012.

[8] Y. W. Li and C. Kao, "An accurate power control strategy for power-electronics-interfaced distributed generation units operating in a low-voltage multibus microgrid," *IEEE Trans. Power Electron.*, vol. 24, no. 12, pp. 2977–2988, Dec. 2009.

[9] D. N. Zmood, D. G. Holmes, and G. H. Bode, "Frequency-domain analysis of three-phase linear current regulators," *IEEE Trans. Ind. Appl.*, vol. 37, no. 2, pp. 601–610, Mar./Apr. 2001.

[10] S. M. Ali and M. P. Kazmierkowski, "Pwm voltage and current control of four-leg vsi," in *Industrial Electronics, 1998. Proceedings. ISIE '98. IEEE International Symposium on*, vol. 1, Jul 1998, pp. 196–201 vol.1.

[11] L. Matakas, W. P. S. Junior, and A. R. Giaretta, "Minimizing current ripple in 3-phase, 4-wire, voltage source converter by injection of an optimal zero sequence signal," in *Proc. of Ninth Brazilian Power Electronics Conference (COBEP 07)*, Blumenau, 2007, pp. 395–400.

[12] S. Buso and P. Mattavelli, *Digital Control in Power Electronics*, 1st ed., J. Hudgins, Ed. United States: Morgan & Claypool, 2006.

[13] D. G. Holmes, T. A. Lipo, B. P. McGrath, and W. Y. Kong, "Optimized design of stationary frame three phase ac current regulators," *IEEE Trans. Power Electron.*, vol. 24, no. 11, pp. 2417–2426, Nov 2009.

[14] P. H. I. Hayashi and L. Matakas, "Decoupled stationary abc frame current control of three-phase four-leg four-wire converters," in *2017 Brazilian Power Electronics Conference (COBEP)*, Nov 2017, pp. 1–6.

[15] P. Tenti, J. L. Willems, P. Mattavelli, and E. Tedeschi, "Generalized symmetrical components for periodic non-sinusoidal three-phase signals," in *Proc. of Seventh International Workshop on Power Definitions and Measurements under Non-Sinusoidal Conditions*, Cagliari, Jul. 2006, pp. 1–7.

[16] J. G. Hwang, P. W. Lehn, and M. Winkelnkemper, "A generalized class of stationary frame-current controllers for grid-connected ac-dc converters," *IEEE Trans. Power Del.*, vol. 25, no. 4, pp. 2742–2751, Oct 2010.

[17] L. L. H. Costa, P. J. A. Serni, and F. P. Marafao, "An analysis of generalized symmetrical components in non sinusoidal three phase systems," in *XI Brazilian Power Electronics Conference*, Sept 2011, pp. 502–507.

[18] A. Reznik, M. G. Simoes, A. Al-Durra, and S. M. Muyeen, "Lcl filter design and performance analysis for grid-interconnected systems," *IEEE Trans. Ind. Appl.*, vol. 50, no. 2, pp. 1225–1232, Mar./Apr. 2014.

[19] P. Tenti, H. K. M. Paredes, and P. Mattavelli, "Conservative power theory, a framework to approach control and accountability issues in smart microgrids," *IEEE Trans. Power Electron.*, vol. 26, no. 3, pp. 664–673, Mar. 2011.

[20] M. C. B. P. Rodrigues, P. C. S. Furtado, C. R. B. S. Rodrigues, R. A. F. Ferreira, A. A. Ferreira, P. G. Barbosa, and H. A. C. Braga, "Development of a small-signal model for a two-phase three-wire active power filter," in *2017 Brazilian Power Electronics Conference (COBEP)*, Nov 2017, pp. 1–7.